

## Impedance spectroscopy studies of surface engineered TiO<sub>2</sub> nanoparticles using slurry technique

SASIDHAR SIDHABATTUNI<sup>1\*</sup>, SRI HARSHA AKELLA<sup>1</sup>, ABILASH GANGULA<sup>1</sup> and SANDEEP PATNAIK<sup>2</sup>

<sup>1</sup>Sri Sathya Sai Institute of Higher Learning (Deemed to be University), Department of Chemistry, Prasanthi Nilayam, Andhra Pradesh 515 134, India

<sup>2</sup>Sri Sathya Sai Institute of Higher Learning (Deemed to be University), Department of Physics, Prasanthi Nilayam, Andhra Pradesh 515 134, India

MS received 30 March 2015; accepted 4 June 2015

**Abstract.** Dielectric analysis of nanometre range size ceramic particles like TiO<sub>2</sub> is very important in the understanding of the performance and design of their polymer nanocomposites for energy storage and other applications. In recent times, impedance spectroscopy is shown to be a very powerful tool to investigate the dielectric characteristics of not only sintered and/or pelleted ceramic materials but also particulates/powders (both micron-sized and nano-sized) using the slurry technique. In the present work, impedance spectroscopy employing slurry methodology was extended to study the influence of various chemical groups on the nano-TiO<sub>2</sub> surface on the electrical resistivity and the dielectric permittivity of nanoparticles. In this regard, different organophosphate ligands with linear, aromatic and extended aromatic nature of organic groups were employed to remediate the surface effects of nanoTiO<sub>2</sub>. It was observed that the type of chemical nature of surface engineered nanoparticles' surface played significant role in controlling the surface electrical resistivity of nanoparticles. Surface passivated nanoTiO<sub>2</sub> yielded dielectric permittivity of about 70–80, respectively.

**Keywords.** Impedance; nanoTiO<sub>2</sub>; self-assembled monolayers; electrical resistivity; permittivity.

### 1. Introduction

Titanium dioxide (TiO<sub>2</sub>) has been extensively studied in electronic applications, including type I capacitors, multi-layered ceramic capacitors (MLCCs), low-temperature Co-fired ceramic (LTCC) substrate and varistors. Relatively high dielectric constant ( $\epsilon_r \sim 100$ ) at room temperature and high dielectric breakdown strength ( $> 100 \text{ kV cm}^{-1}$ ) are responsible for its applications as capacitors.<sup>1</sup> Research studies showed that nanostructured TiO<sub>2</sub> ceramics possess significantly higher dielectric breakdown strength than coarse grain TiO<sub>2</sub> ceramics, making them promising candidate materials for designing high-energy density capacitors.<sup>2</sup> Moreover, with the miniaturization of electronic devices, the downsizing of MLCCs and the use of nanocomposites like 0–3 polymer–ceramic nanocomposites has been accelerated for designing future generation energy storage capacitors.<sup>3–5</sup> Because the dielectric constant is an intrinsic property of a material, quantifying  $\epsilon_r$  of nano-sized ceramic particles like TiO<sub>2</sub> is very important for predicting and designing the dielectric properties of their nanocomposites in polymer matrices for capacitors, MLCCs and other applications.

Impedance spectroscopy is a powerful technique to study electrical and dielectrical responses of ceramic materials. Traditionally, sintered ceramic discs are prepared to characterize bulk dielectric properties of ceramics. However, the dielectric properties of the loose particulate powders, especially nano-sized dielectric particles, significantly differ from that of a bulk material due to high surface energy and surface conductivity of ceramic nanoparticles. Hence, it is very difficult to obtain the 'nano-size effect' of the ceramic nanoparticles' dielectric response by using the traditional solid-state pellet technique. Hence, dielectric characterization of nanoparticles requires the development of reliable and reproducible measurement techniques.<sup>2,6,7</sup> The slurry approach which involves dispersion of particles in a liquid is a common method to measure the capacitance of the slurry from which the permittivity of particles can be calculated. Generally, the capacitance of the slurry, measured at a single frequency, is used to calculate the permittivity of the particles by applying finite element models.<sup>8–12</sup> In the recent research studies, impedance spectroscopy was applied to determine the permittivity of dielectric particles through impedance analysis of slurries, where dielectric particles to be characterized were suspended in a lossy liquid. The particles' dielectric properties were then extracted from low-frequency spectra using equivalent circuit models.<sup>6,12–18</sup>

\*Author for correspondence (siddabattunisidhar@sssihl.edu.in)

While the slurry methodology has been demonstrated for a variety of metal oxide ceramic powders, it was shown to be applicable for micron-sized particles but not for nanoparticles due to the surface conductivity and surface energy effects of the nanoparticles compounded by the large surface area of nanoparticles.<sup>6,19</sup> However, in our earlier works, the particle slurry impedance spectroscopy technique was shown to be effective in characterizing the dielectric permittivity of nano-sized ceramic particles like BaTiO<sub>3</sub> and TiO<sub>2</sub> as well by the application of a self-assembled monolayer (SAM) onto the nanoparticle as a surface passivation layer that mitigates the surface conductivity and the surface energy effects of the nanoparticles.<sup>19,20</sup>

Surface treatment of nanoparticles is very crucial in the field of polymer nanocomposites with regard to compatibility and quality of dispersion of inorganic nanoparticles in organic polymer matrices.<sup>5,20</sup> Hence, care should be taken in selecting the appropriate surface modifying agents, suitable for the intended application of polymer nanocomposites. In this present work, the use of impedance spectroscopy using the slurry technique for studying the influence of chemical nature of the nanoTiO<sub>2</sub> particles on its electrical resistivity and dielectric permittivity was extended. In this regard, the surface of the titania nanoparticles were modified using various organophosphate coupling agents to mitigate the surface effects. Unlike the earlier work where various functionalized aromatic organophosphates were used, here different organophosphate ligand molecules containing linear, aromatic and extended aromatic chemical groups were employed. Figure 1 shows the chemical structures of organophosphate ligands that were examined as filler surface modifying ligands.

## 2. Experimental

Commercially available nanoTiO<sub>2</sub> powder (>99%, 10–25 nm APS, and 200–240 m<sup>2</sup> g<sup>-1</sup>) was obtained from US Research Nano Materials Inc., Texas, USA and used as is

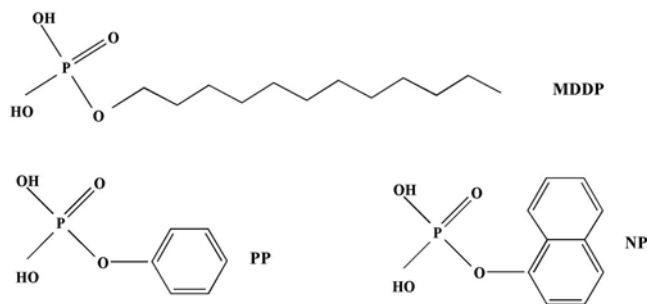


**Figure 1.** Molecular structures of organophosphate ligands: monododecylphosphate (MDDP), phenyl phosphate (PP) and 1-naphthyl phosphate (NP) used to modify the surface of nano-TiO<sub>2</sub>.

in the preparation of slurries in the host liquid, butoxyethanol (BOE) (>99%; Sigma Aldrich, USA,  $\epsilon_r \sim 10$ ). Organophosphate surface modifying agents, monododecyl phosphate (MDDP) and phenyl phosphate (PP), were obtained from TCI Chemicals (India) Pvt. Ltd. and 1-naphthyl phosphate (NP) was obtained from Sigma Aldrich, USA.

In a typical surface modification reaction, TiO<sub>2</sub> nanoparticles were dispersed in suitable solvent. Organophosphate ligand, approximately 10–15 wt% of particle mass was mixed with a nanotitania dispersion and stirred at reflux conditions for 18–24 h. The surface modified nanoTiO<sub>2</sub> powder was then isolated and purified by washing through repeated centrifugation and re-dispersion in solvent for 4–5 times to remove any excess and/or physisorbed ligands. The surface-treated TiO<sub>2</sub> nanoparticles were dried thoroughly at 160°C for 6–10 h before weight loss studies using thermogravimetry (TGA) and the preparation of slurries in BOE for impedance characterization. Water (distilled and deionized) was used as dispersion medium for surface functionalization using PP and MDDP. Methanol was used as dispersion medium for surface functionalization using NP.

Before preparing the slurry samples of surface modified and unmodified nanoTiO<sub>2</sub> powders for impedance studies, samples were characterized using TGA and X-ray photoelectron spectroscopy (XPS). TGA (Mettler Toledo TGA/DSC 1) was used to measure the mass of organophosphate incorporated on the surface of nanoparticles. The number of phosphate groups located per surface area of particles may be estimated from the surface area per mass unmodified TiO<sub>2</sub> nanoparticles and mass organophosphate per mass particle.<sup>5,21</sup> Sample weight loss was measured from ambient to 800°C at 10°C min<sup>-1</sup> in air. XPS (AxisUltra DLD, Kratos Analytical UK with AlK $\alpha$  as the radiation source) was utilized for determining the chemical composition of the particle surfaces of various nanoTiO<sub>2</sub> powders.

The impedance slurry samples were prepared by dispersing dried nanoparticles (20 vol% particle concentration) in BOE using ultrasound (Microson ultrasonic cell disruptor, Misonex Incorporated, NY; tapered 2 mm microtip) for a maximum of 1 min at a 50% output power before impedance spectroscopy measurement. Stainless electrodes (surface area ( $A$ ) is about 3 cm<sup>2</sup> and separation distance ( $L$ ) of about 1.5 mm) were assembled as a sample measurement cell. Ivium Compact Stat (Ivium Technologies, Netherlands) was used to collect the impedance data in the frequency range of 1 Hz–1 MHz and voltage amplitude of 100 mV.

An equivalent circuit approach with two RC elements connected in series was used to extract quantitative information, such as the permittivity of dielectric particles, from the impedance spectra of the slurries as described earlier.<sup>19</sup> Z-view software (Scribner Inc., Southern Pines, NC) was used to fit the spectra with the equivalent circuit

model and to calculate the parameters within the equivalent circuit. The accuracy and the limitations of this impedance spectroscopy using the slurry technique have been discussed in the previous investigations.<sup>12–17,19</sup> A selected list from those investigations are: low-frequency characterization technique has better accuracy and reliability for high dielectric contrast mixtures (as in the present study), while other high frequency techniques are preferable for low dielectric contrast mixtures; particle size itself does not influence the impedance spectra, although particle properties are size dependent; it is desirable to have the solids loading higher than 10% for greater particle signal, but which is limited by percolation threshold that influences dispersion quality, including the presence of air voids and particle gravimetric settling; dielectric permittivity characterization is almost constant for different particle volume concentrations; unlike micro-particle slurries, nanoparticle slurries are stable and not susceptible to settling and thus does not influence the dielectric characterization results.

### 3. Results and discussion

Organophosphate ligand species are capable of forming a strong, stable, complexed SAMs on metal oxides surface,<sup>22,23</sup> including TiO<sub>2</sub>. The SAM layer via phosphate bridging can passivate the surface by chemically insulating the particle, similar to that employed with corrosion inhibitors.<sup>24</sup> After treating the nanotitania filler surface with organophosphate ligands, prior to the impedance measurements, the nanoparticles were first assessed for quantity of organic groups bonded via phosphate groups on the particle surface using TGA. TGA analysis of surface modified and unmodified nanoTiO<sub>2</sub> particles are shown in figure 2 and table 1. Significant organic weight loss observed above 200°C for the organophosphate ligand-modified TiO<sub>2</sub> nanoparticles was attributed mainly to thermal decomposition and volatilization of organic residues.<sup>21,25,26</sup> The surface group density was calculated after removing mass losses assigned to bare nanoTiO<sub>2</sub>, before surface modification. Surface group density was then calculated from mass loss and particle surface area per mass of bare TiO<sub>2</sub>, which is similar in method reported earlier for surface modification of metal oxides.<sup>5</sup>

Organic weight loss of MDDP- and PP-treated nanoTiO<sub>2</sub> particles correspond to a surface group density of about one organophosphate molecule per nm<sup>2</sup> (table 1). Surface group density was about one-fourth that of the theoretical assumption of surface group density of organophosphonate groups per nm<sup>2</sup> for highly ordered SAMs.<sup>27</sup> A polycrystalline surface nature of nanosized metal-oxide particles and the possibility of multi-dentate bonding for the phosphate groups on metal oxide surfaces may be responsible for relatively less ordered SAM surfaces.<sup>5,22</sup>

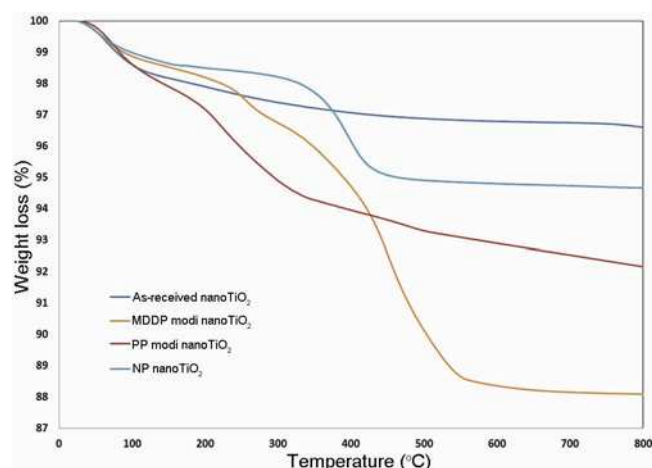


**Figure 2.** Thermogravimetric analysis curves of surface modified and unmodified TiO<sub>2</sub> nanoparticles.

Unlike MDDP- and PP-treated nanoTiO<sub>2</sub>, NP-modified nanoTiO<sub>2</sub> particles surface group density was only about half a organophosphate molecule per nm<sup>2</sup>, which is attributed mainly to the pronounced steric effect offered by the aryl groups (naphthyl) of NP.

XPS measurements (table 2) indicate the introduction of phosphorus groups on the surface modified nanoTiO<sub>2</sub> samples. The binding energy of oxygen atoms of surface hydroxyl groups overlaps with the organophosphate ligands on the nanoTiO<sub>2</sub> surface.<sup>20,28,29</sup> The XPS scans of the O(1s) region of nanoTiO<sub>2</sub> in comparison to surface-treated nanoTiO<sub>2</sub> are shown in figure 3. Binding electrons at 530.5 eV (literature values range from 529.9 to 530.9 eV)<sup>29</sup> correspond to the oxygen atoms due to Ti–O bond of TiO<sub>2</sub>. But figure 3a indicates major portion of the oxygen region of nanoTiO<sub>2</sub> at 532.8 eV compared to the oxygen region that corresponds to Ti–O bond of TiO<sub>2</sub>. This is mainly attributed to the presence of high concentration of surface hydroxyl (OH) groups available due to high surface area of nano-sized TiO<sub>2</sub> particles. A small peak at 535.1 eV is attributed to chemisorbed water.<sup>28</sup> In comparison, surface modified powders, mainly MDDP- and PP-modified nanoTiO<sub>2</sub> (figure 3b and c, respectively), showed a distinct peak at 530.5 eV that corresponds to the oxygen due to Ti–O bond, indicating the surface reaction of hydroxyl groups of nanoTiO<sub>2</sub> with organophosphate ligands and the O(1s) region ranging from 532 to 534 eV corresponds to the oxygen atoms of phosphonyl oxygen (P=O), phosphoryl oxygen (P–O) and R–O–P bonds, where R is alkyl or aryl (phenyl, naphthyl) carbon, of organophosphate ligands.<sup>20,28,29</sup> NP-modified nanoTiO<sub>2</sub> (figure 3d) showed a broad peak but not a distinct peak at 530.5 eV, indicating lower surface group density of NP groups on nanoTiO<sub>2</sub> surface, mainly attributed due to the steric hindrance of aryl groups of NP ligand. TGA analysis also showed comparatively low surface group density for NP-modified nanoTiO<sub>2</sub>.

**Table 1.** TGA data of surface modified and unmodified TiO<sub>2</sub> nanoparticles.

Powder	TGA		
	Organic weight loss (%)	Grafting density (groups nm <sup>-2</sup> )	Grafting density (Å <sup>2</sup> molecule <sup>-1</sup> )
NanoTiO <sub>2</sub>	0.00	–	–
MDDP-treated nanoTiO <sub>2</sub>	8.88	1.11	90
PP-treated nanoTiO <sub>2</sub>	4.30	0.83	120
NP-treated nanoTiO <sub>2</sub>	2.87	0.41	245

**Table 2.** XPS measurement data of surface modified and unmodified TiO<sub>2</sub> nanoparticles.

Powder	XPS (atomic per cent)			
	C (1s)	Ti (2p)	O (1s)	P (2p)
NanoTiO <sub>2</sub>	37.66	3.07	59.27	0
MDDP nanoTiO <sub>2</sub>	34.89	9.58	53.05	2.48
PP nanoTiO <sub>2</sub>	42.23	6.44	49.37	1.96
NP nanoTiO <sub>2</sub>	45.54	4.80	47.34	2.32

After both the TGA and the XPS measurements of surface modified nanoTiO<sub>2</sub> powders supported the evidence of surface bonding by organophosphate ligands onto the nanoTiO<sub>2</sub> surface, impedance spectroscopy of the powder samples using the slurry technique were carried out. Summary of the impedance spectra of the nanoTiO<sub>2</sub>-based powder slurries in BOE host liquid is shown in figure 4. The impedance spectra ( $Z''$  vs.  $Z'$ , where  $Z'$  and  $Z''$  are the real and imaginary parts of the impedance) of the particles' slurries were subjected to equivalent circuit modelling to deconvolute the solvent element contributions from particle element contributions using two RC elements (figure 4). Four parameters, high-frequency resistance ( $R1$ ) and capacitance ( $C1$ ) corresponding to the liquid portion of the slurries and low-frequency resistance ( $R2$ ) and constant phase element ( $CPE2$ ) corresponding to the particle portion of the slurries obtained for each impedance spectrum and their calculated dielectric permittivities of individual components of the slurries are reported in table 3.

In the impedance spectra of the slurries, the distinctiveness of the relaxation events and their corresponding semicircle patterns of the individual components of the slurries are sensitive to the dielectric contrast between the individual components and insensitive to the resistivity of the host liquid.<sup>12</sup> Therefore, greater the dielectric contrasts, more distinct are the semicircles of the slurry components. Two distinct relaxation events are possible with two distinct semicircles if micron-sized particles like BaTiO<sub>3</sub> are employed in host BOE liquid, due to huge dielectric contrast. However, due to the reduced dielectric contrast between the nanoparticles like TiO<sub>2</sub>, BaTiO<sub>3</sub> and the host liquid, impedance spectra of the TiO<sub>2</sub> slurries in BOE showed only one elongated semicircle (figure 4). Loading of the host liquid with ceramic particles increases

its dielectric constant slightly as the liquid is substituted with material of higher dielectric constant.<sup>19</sup>

When bare nanoTiO<sub>2</sub> particles are added to the host liquid, the electrical resistivity ( $\rho = R \times A/L$ ) of the host liquid ( $R1$ ) reduced from 4.78 to 2.18 kΩ m and the dielectric permittivity of bare nanoTiO<sub>2</sub> ( $\epsilon_r \sim 41$ ) was not reliably obtained. As the change in resistivity of host liquid cannot influence the dielectric permittivity of particles,<sup>12</sup> lower resistivity of the liquid portion and lower dielectric permittivity of the particle portion observed should be from the particles' nature and can be mainly attributed to the higher surface energy and surface conductivity of the nanoTiO<sub>2</sub> particles. The origin of the particle surface conductivity and higher surface energy of nanoTiO<sub>2</sub> can be attributed to its ionic surface charge,<sup>30</sup> under-coordinated Ti ions and oxygen vacancies.<sup>31–33</sup> Higher the under-coordinated positions, higher is the surface energy.<sup>31,32</sup> Thus, reduction in the resistivity of host liquid and increase in its dielectric constant than usual can be attributed to significant concentration of contaminants through dissolution or desorption or migration of ions from the particles surface into the solvent environment during dispersion of nanoparticles in the host liquid.<sup>19</sup>

Change in resistivity of host liquid was either lowered or even further improved than host liquid, depending on the type of chemical nature at the liquid–particle interface, when the surface modified nanoTiO<sub>2</sub> particles were employed for the impedance measurement of the slurries. This improvement in solvent impedance (table 3 and figure 4) is mainly attributed to the presence of the SAM layer, which appears to offer surface chemical passivation properties via phosphate group on to the particle surface to prevent conductive species from dissolving/desorbing from the particle surface into the solvent.<sup>19</sup> It was observed that the resistivity of surface modified nanoTiO<sub>2</sub> ( $R2$ ) was either lowered or improved than unmodified nanoTiO<sub>2</sub>. MDDP-treated nanoTiO<sub>2</sub> was observed to result in 50% reduction in the resistivity, whereas PP- and NP-treated nanoTiO<sub>2</sub> were observed to result in about 100 and 150% increase in the resistivity as compared to untreated nanoTiO<sub>2</sub>. Improvement in the electrical resistivity of host solvent and particle resistivity was observed to be in the order of MDDP < PP < NP. These differences in the electrical resistance and resistivity of the solvent

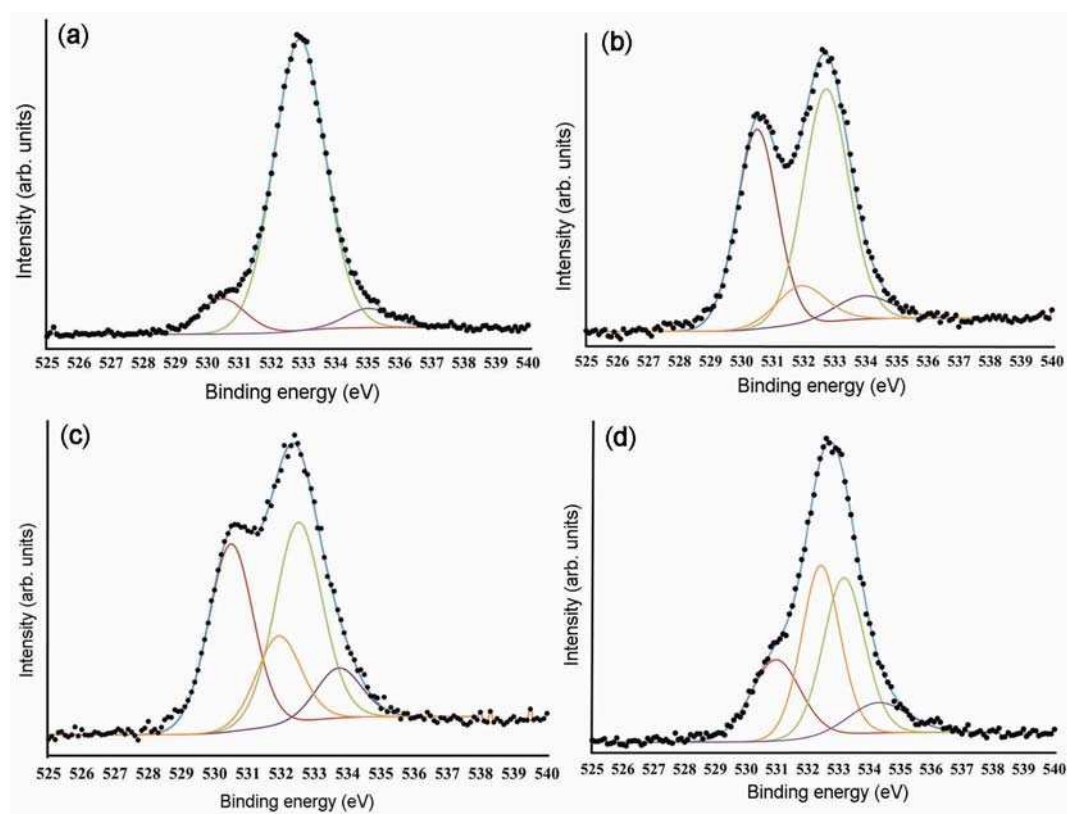


**Figure 3.** XPS scans of O(1s) region of (a) nanoTiO<sub>2</sub>, (b) MDDP nanoTiO<sub>2</sub>, (c) PP nanoTiO<sub>2</sub> and (d) NP nanoTiO<sub>2</sub> samples. Dotted line shows the raw data points that are plotted with continuous line deconvoluted and fitting summation curves.

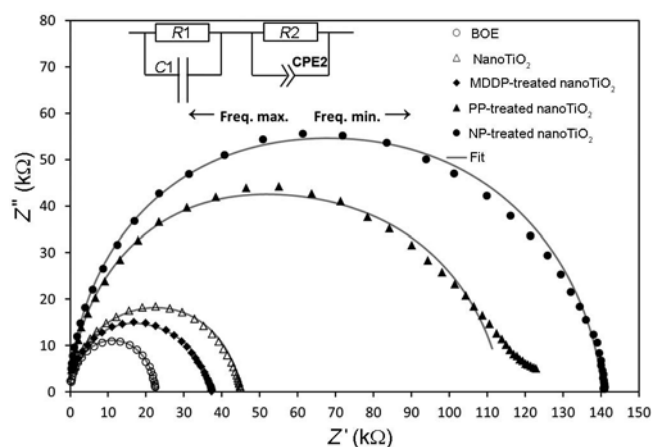


**Figure 4.** Impedance spectra of 20 vol% nanoTiO<sub>2</sub>-based powders' slurries in BOE fluid, plotted in comparison with the impedance spectrum of the host liquid BOE.

impedance and particle impedance for various surface functionalized nanoTiO<sub>2</sub> slurries are attributed to the difference in the chemical nature of functional group ligands employed. Alkyl group of the linear MDDP chemical group is traditionally known to be electron donating in electronic nature, whereas phenyl chemical group of the

aromatic PP and aryl (1-naphthyl) chemical group of the extended aromatic group of the NP are traditionally known to be relatively electron withdrawing in electronic nature.<sup>34</sup> That is, resistivity of the particles and the solvent is observed to be comparatively higher when aromatic and extended aromatic chemical groups are present on the particle surface. Even lower surface group density of SAMs in NP-treated nanoTiO<sub>2</sub> in comparison to PP- and MDDP-treated nanoTiO<sub>2</sub> appears to greatly enhance the resistivity of particle surface. Hence, it appears that the choice of chemical nature of ligands employed for surface passivation of metal oxide nanoparticles plays an important role in altering the particle surface electrical resistivity.

Unlike the bare nanoTiO<sub>2</sub>, the effective dielectric permittivities of about 70–80 of the surface-treated nanoTiO<sub>2</sub> particles, calculated from the equivalent circuit modelling of the impedance spectra, appears to be of reasonable values (table 3). The choice of organic functional group did not seem to influence the dielectric permittivity of nanoTiO<sub>2</sub> to a significant extent. Aryl (phenyl, naphthyl) groups which contains polarizable  $\pi$  ( $\pi$ ) electrons is known to have a small, permanent dipole moment and thus relatively more polarizable than simple alkyl group.<sup>35</sup> After considering the differences in the surface group

**Table 3.** Fitting parameters of the impedance data and the permittivity values of the samples.

Sample	R1 (k $\Omega$ )	C1 (F)	R2 (k $\Omega$ )	CPE2-T (F)	CPE2-P	C2 (F)	$\epsilon_r^a$	$\epsilon_r^b$
BOE	23.9	3.1E-11	–	–	–	–	10.7	–
NanoTiO <sub>2</sub>	10.9	9.9E-11	33.9	3.27E-10	0.90	9.7E-11	42.1	41.3
MDDP nanoTiO <sub>2</sub>	17.4	6.1E-11	19.8	8.94E-10	0.87	1.7E-10	25.7	72.3
PP nanoTiO <sub>2</sub>	46.9	6.6E-11	67.0	7.25E-10	0.88	1.9E-10	28.1	80.6
NP nanoTiO <sub>2</sub>	56.7	6.3E-11	83.7	3.99E-10	0.92	1.6E-10	26.7	70.7

<sup>a</sup>Permittivity of liquid component of the slurry.

<sup>b</sup>Permittivity of particulate component of the slurry.

densities, relatively similar or little improvement in the dielectric permittivity values observed for NP- and PP-treated nanoTiO<sub>2</sub> compared to MDDP-treated nanoTiO<sub>2</sub> may be attributed to the small differences in the polarizability between the alkyl, phenyl and naphthyl groups employed on the particles' surface.

Study on the influence of additional polar functional groups like amide, nitrile, etc. on the electrical resistivity and dielectric permittivity of nanoTiO<sub>2</sub> compared to non-polar functional groups will be studied in our future work. In addition, the influence of improved surface resistivity of nanoparticles on the dielectric properties like dielectric breakdown strength and corresponding energy storage densities of the 0–3 polymer–TiO<sub>2</sub> nanocomposites will be studied and reported in the future work.

#### 4. Conclusions

Surface passivation using the SAM approach and the choice of chemical nature of functional group on ceramic nanoparticles surface appear to be the important tools that can remove or remediate surface lattice vacancies, lower the surface energy, and alter the dielectric and impedance characteristics of metal oxide nanoparticles. Comparison of the impedance spectra of nanoTiO<sub>2</sub>-based slurries in host liquid showed improved electrical resistivity of titania particles when aromatic and extended aromatic chemical groups are preferred compared to linear alkyl groups. In addition, surface passivated nanoTiO<sub>2</sub> powders yielded a reliable and reproducible permittivity values in the range of 70–80.

#### Acknowledgements

This work was made possible by the funds provided by the DST-SERB Start-Up Research Grant for Young Scientists (No. SB/FT/CS-019/2012), Government of India. We would like to acknowledge Dr Vladimir Petrovsky from Missouri University of Science and Technology, USA, for his assistance in equivalent circuit modelling and the Micro and Nano Characterization Facility of the Centre for Nano Science and Engineering, Indian Institute of Science, Bangalore, for providing XPS characterization.

#### References

- Marinel S, Choi D H, Heuguet R, Agrawal D and Lanagan M 2013 *Ceram. Int.* **39** 299
- Chao S, Petrovsky V and Dogan F 2010 *J. Am. Ceram. Soc.* **93** 3031
- Wada S, Kondo S, Moriyoshi C and Kuroiwa Y 2008 *Jpn. J. Appl. Phys.* **47** 7612
- Tsurumi T, Sekine T, Kakemoto H, Hoshina T, Nam S-M, Yasuno H and Wada S 2006 *J. Am. Ceram. Soc.* **89** 1337
- Siddabattuni S, Schuman T P and Dogan F 2011 *Mater. Sci. Eng. B* **176** 1422
- Petrovsky V, Petrovsky T, Kamlapurkar S and Dogan F 2008 *J. Am. Ceram. Soc.* **91** 1814
- Chang K C, Yeh Y C and Lue J T 2012 *Measurement* **45** 808
- Wada S, Yasuno H, Hoshina T, Nam S-M, Kakemoto H and Tsurumi T 2003 *Jpn. J. Appl. Phys.* **42** 6188
- Wada S, Hoshino T, Yasuno H, Ohishi M, Kakemoto H, Tsurumi T and Yashima M 2005 *Ceram. Eng. Sci. Proc.* **26** 89
- Tsurumi T, Sekine T, Kakemoto H, Hoshina T, Nam S-M, Yasuno H and Wada S 2005 *Mater. Res. Soc. Symp. Proc.* **833** 243
- Manohar A and Dogan F 2005 *Ceramic transactions, advances in electronic and electrochemical ceramics* (eds) F Dogan and P Kumta (Westerville, OH: The American Ceramic Society) p 93
- Petrovsky V and Dogan F 2009 *J. Am. Ceram. Soc.* **92** 1054
- Petrovsky V, Petrovsky T, Kamlapurkar S and Dogan F 2008 *J. Am. Ceram. Soc.* **91** 1817
- Petrovsky V, Manohar A and Dogan F 2006 *J. Appl. Phys.* **100** 014102-1
- Petrovsky V, Petrovsky T, Kamlapurkar S and Dogan F 2008 *J. Am. Ceram. Soc.* **91** 3590
- Jasinski P, Petrovsky V and Dogan F 2010 *J. Appl. Phys.* **108** 074111-1
- Petrovsky V, Jasinski P and Dogan F 2012 *J. Appl. Phys.* **112** 034107-1
- Zhou W, Hinojosa B B and Nino J C 2012 *J. Am. Ceram. Soc.* **95** 457
- Siddabattuni S, Schuman T P, Petrovsky V and Dogan F 2013 *J. Am. Ceram. Soc.* **96** 1490
- Siddabattuni S, Schuman T P and Dogan F 2013 *ACS Appl. Mater. Interfaces* **5** 1917
- Porkodi K and Arokiamary S D 2007 *Mater. Charact.* **58** 495
- Schuman T P, Siddabattuni S, Cox O and Dogan F 2010 *Compos. Interface* **17** 719
- Mutin P H, Guerrero G and Vioux A 2005 *J. Mater. Chem.* **15** 3761

24. Gao W, Dickinson L, Grozinger C, Morin F G and Reven L 1996 *Langmuir* **12** 6429
25. Reid D L, Russo A E, Carro R V, Stephens M A, LePage A R, Spalding T C, Petersen E L and Seal S 2007 *Nano Lett.* **7** 2157
26. Geng H, Peng R, Han S, Gu X and Wang M 2010 *J. Electron. Mater.* **39** 2346
27. Helmy R and Fadeev A Y 2002 *Langmuir* **18** 8924
28. Moreno-Castilla C, Maldonado-Hódar F J, Carrasco-Marín F and Rodríguez-Castellón E 2002 *Langmuir* **18** 2295
29. Viornery C, Chevotot Y, Léonard D, Aronsson B-O, Péchy P, Mathieu H J, Descouts P and Grätzel M 2002 *Langmuir* **18** 2582
30. Leroy P, Tournassat C and Bizi M 2011 *J. Colloid Interface Sci.* **356** 442
31. Fernandez-Garcia M and Rodriguez J A 2009 *Nanomaterials: inorganic and bioinorganic perspectives* (eds) C M Lukehart and R A Scott (New York: Wiley) p 453
32. Lazzeri M, Vittadini A and Selloni A 2001 *Phys. Rev. B* **63** 155409
33. Zhang H and Bandfield J F 1998 *J. Mater. Chem.* **8** 2073
34. Macomber R 1996 *Organic chemistry* (California, CA: University Science Books) Vol 1, p 267
35. Chester T L and Pinkston J D 2005 *Analytical instrumentation handbook* (ed) J Cazes (New York: Marcel Dekker) 3rd ed, p 759